Quantum resonances in the valence band of zinc-blende semiconductors. II. Results for p-InSb under uniaxial stress

R. Ranvaud*
Hochfeldmagnetlabor Grenoble, France

H.-R. Trebin†
Institut für Theoretische Physik, Universität Regensburg, Federal Republic of Germany

U. Rössler
Institut für Theoretische Physik, Universität Regensburg und Max-Planck-Institut für Festkörperforschung, Stuttgart, Federal Republic of Germany

Fred H. Pollak‡
Department of Physics, Belfer Graduate School of Science, Yeshiva University, New York 10033
(Received 19 October 1978)

Quantum resonances in the valence bands of p-type InSb have been measured in a far-infrared resonance (FIR) experiment and interpreted using previously developed theory. Both cyclotron- and combined-resonance spectra were studied under uniaxial stress (parallel to the magnetic field) in the [001] and [111] direction. Since in the FIR experiment the quantum resonances are observed at much higher magnetic fields than by use of microwaves, the experimental arrangement was tested by studying quantum resonances in p-type Ge. Using the band parameters of Hensel and Suzuki the data for this material can be quantitatively explained with a theory that works in the Kane model, thus taking into account exactly the strong coupling between the upper valence band and the lowest conduction band owing to the high magnetic fields. The fundamental transitions in p-type InSb show a peculiar dependence on the strength and direction of the uniaxial stress, which is due to stress-induced $\vec{k}$-linear terms. The observed cyclotron and combined resonances are quantitatively explained in the framework of the theory developed previously and a set of band parameters for InSb is derived.

I. INTRODUCTION

Cyclotron-resonance experiments in semiconductors belong to the most direct and powerful methods to determine effective-mass parameters of electrons and holes. The complex valence-band structure of diamond- and zinc-blende-type semiconductors gives rise to deviations from the "classical" cyclotron resonance of light and heavy holes if transitions between the lowest Landau levels are studied. These quantum effects, which were predicted by Luttinger and Kohn,[1,2] manifest themselves in very complex resonance spectra that, however, can be disentangled by applying uniaxial stress. Experiments of this kind were carried out and quantitatively interpreted for the first time by Hensel and Suzuki (HS)[3-5] for Ge. A set of high-precision effective-mass parameters was derived from an analysis of the so-called fundamental transitions, for which the resonant magnetic field is almost independent of the applied stress.[5] These cyclotron-resonance experiments have been performed for Ge at microwave frequencies with the carriers being generated in the sample by white light. The great success of this experiment suggested the application of the method also to other materials in order to obtain band parameters of high accuracy.

In unstressed p-type InSb cyclotron resonance was observed by mm-wavelength light[6] and microwave absorption[7,8] without any evidence of a complex spectrum due to quantum effects. The low quality of III-V material as compared with Ge made experiments at higher frequencies necessary. Thus, it was in a far-infrared experiment using a HCN (337 μm) laser, that quantum effects in the cyclotron resonance of p-type InSb were observed for the first time.[9] Several years later detailed far-infrared resonance (FIR) experiments on p-type InSb with uniaxial stress applied in the [001], [111], [110], and [112] directions were performed.[10] Results for the [001] and [111] directions will be presented in this paper. More recently intraband transitions in p-type InSb were investigated also by magneto-Raman scattering[11] and by photoconductivity studies.[12]

In p-type InSb the stress dependence of the fundamental transitions exhibits a behavior different from that of Ge; the resonance magnetic field for these transitions depends on both the direction and the strength of the stress applied.[10] This observation is unexpected in view of existing theories.

Suzuki and Hensel[4] extended Luttinger's theory by including the stress dependence,[13,14] and predicted an almost stress-independent resonance magnetic field for the fundamental transitions in Ge. Their theory is formulated for the manifold of the $j=3/2$ uppermost valence-band states. An extension of Pidgeon and Brown's (PB) theory[15,16] [which applies to the eightfold space of the lowest conduction band and the spin-orbit split valence band (Kane model)] to include the effects of strain[10] also failed to explain the observed stress dependence of the fundamental transitions in p-type InSb. It was suggested[10] and later on verified[17] that this behavior is caused by stress-induced k-linear terms, which occur in zinc-blende compounds due to inversion asymmetry. Thus it became necessary to modify existing theories of Landau levels[2,4,15,16] to include stress-dependent terms of tetrahedral symmetry.

In order to develop a more complete theory the $\vec{k}\cdot\vec{p}$ interaction was treated within the eightfold space of the Kane model. We were led to this extension, since a first attempt to complete Suzuki and Hensel's[4] effective-mass Hamiltonian by such terms failed for transitions at higher resonance magnetic fields ($H>50$ kG), even though third-order projections onto the space of $j=3/2$ states were taken into account. The failure can be ascribed to the strong coupling between valence- and conduction-band states due to the small gap. In the preceding paper,[18] henceforth denoted I, we developed a theory with the following properties: (a) it contains all relevant terms of tetrahedral symmetry; (b) it allows a rigorous classification of Landau levels and formulation of selection rules for inter- and intraband transitions on purely group-theoretical grounds. On the basis of this theory the observed stress dependence of the cyclotron and combined resonances in p-type InSb is explained quantitatively and a set of band parameters (Luttinger's inverse mass parameters and deformation potentials) is obtained in the present paper. Our values of the Luttinger parameters are about 25% larger than those found by other authors.[19]

As a test of the reliability of a FIR experiment we first present quantum resonances of p-type Ge under uniaxial stress. Due to the higher energy of the HCN laser as compared to the microwave source used in Hensel and Suzuki's[5] experiment, the resonance magnetic fields here are an order of magnitude larger than in Ref. 5. Nevertheless, a complete quantitative interpretation of the FIR data for Ge is possible with the HS band parameters.[5]

The present paper contains the following sections. In Sec. II we give a quantitative description of valence bands and of Landau levels in uniaxially stressed InSb in order to demonstrate the origin of the stress-induced k-linear terms and their consequences. This section provides a qualitative description of the stress dependence of the fundamental cyclotron-resonance and combined resonance transitions. Section III is devoted to experimental details, while Sec. IV contains the experimental results together with the interpretation of the data. In Sec. V we discuss our results in comparison with previous ones.

II. VALENCE-BAND LANDAU LEVELS IN InSb

The general structure of the valence bands of InSb is similar to that of Ge; the hole states at the band edge are fourfold degenerate; a twofold degenerate state is split off by the spin-orbit interaction. In detail, however, there are considerable differences between the band-edge structures, which makes it necessary to extend the theoretical treatment of the Landau levels beyond that of Suzuki and Hensel[4] for Ge.

A. Effective-mass Hamiltonian

The band gap in InSb is direct and sufficiently small ($E_g=0.235$ meV) that the $\vec{k}\cdot\vec{p}$ interaction between the conduction and valence bands produces large nonparabolicities at wave vectors rather close to the center of the Brillouin zone.[20] If—as is the case in the experiments presented here—one penetrates into the valence bands with a HCN laser operating in the far infrared at 337 μm (3.679 meV), this interaction cannot be met by second-order perturbation theory.[21] Also higher-order perturbation theory, e.g., third- and fourth-order projections of the valence–conduction-band $\vec{k}\cdot\vec{p}$ interaction onto the 4×4 space of the uppermost valence-band states, leads to divergences at high magnetic fields or high Landau quantum numbers. Therefore Kane's three-band model has to be employed. In this model the states of the Γ_6 conduction band (labeled by the index c in what follows), of the Γ_8 valence band (index v), and the split-off band Γ_7 (index s) are considered quasi-degenerate and their mutual interaction is taken into account exactly.

In this basis one arrives at an 8×8 effective-mass Hamiltonian matrix[18]

$$\mathcal{H}=\begin{bmatrix}\mathcal{H}^{cc} & \mathcal{H}^{cv} & \mathcal{H}^{cs}\\ \mathcal{H}^{vc} & \mathcal{H}^{vv} & \mathcal{H}^{vs}\\ \mathcal{H}^{sc} & \mathcal{H}^{sv} & \mathcal{H}^{ss}\end{bmatrix}. \tag{1}$$

The inter- and intraband matrices $\mathcal{H}^{\alpha\beta}$, $\alpha,\beta\in\{c,v,s\}$, with inclusion of the magnetic and strain interaction, can be formulated in terms of Pauli

matrices σ_i and ρ_i, $j=\frac{3}{2}$ angular momentum matrices J_i, $i\epsilon\{1,2,3\}$, and 2×4 or 4×2 cross-space matrices T_i and U_i, $i\epsilon\{1,2,3,11,12,33\}$, that have been defined in the preceding paper; the explicit form of the invariant expansion of the blocks $\mathcal{H}^{\alpha\beta}$ ($\mathcal{H}$) is given in paper I (Table IV) together with the necessary notations [Eq. (1) and thereafter].

The strain independent part of the submatrix $\mathcal{H}^{vv}$ is essentially Luttinger's effective-mass Hamiltonian with reduced parameters γ_1, γ_2, γ_3, and κ.[15,16] The k-linear terms, weighted by C, arise from the inversion asymmetry of InSb.[19-21] They cause the Kramers doublets of heavy and light hole bands to split for $\vec{k}\neq\vec{0}$ as discussed by Bell and Rogers.[22] Other constants for the strain independent part of $\mathcal{H}$ are Kane's constants A' and B and the momentum matrix element P between valence and conduction band.

When uniaxial stress is applied, in InSb as in Ge, the Γ_8 valence band, fourfold degenerate at $\vec{k}\neq\vec{0}$, is split due to the reduction of symmetry. This splitting is described by the valence-band deformation potentials D_u and D_u'.[14] The hydrostatic component of the uniaxial stress shifts the valence bands away from the conduction-band edge by an amount proportional to C_1+D_d ($=C_1-a$ in the notation of Pikus and Bir[13]).

A number of terms proportional to the strain tensor components $\epsilon_{\mu\nu}$ are due to the inversion asymmetry of the InSb crystal, and significantly change the Landau spectrum under uniaxial stress as compared to that of Ge. A major part of this paper is concerned with the observation of these terms in quantum resonances; therefore we discuss them separately.

B. Stress-induced k-linear terms

The zone-center states of InSb, in contrast to Ge, do not have a definite parity since the inversion operation is not contained in the crystal point group T_d. Therefore, nonvanishing matrix elements between each pair of Bloch states can exist simultaneously for the $\vec{k}\cdot\vec{p}$ and the strain interaction, whose corresponding operators in Ge have different parity. The combination of the two matrix elements in second-order perturbation theory leads to terms proportional to the product $\epsilon_{\mu\nu}k_\lambda$ of strain-tensor and wave-vector components.

The stress-induced k-linear terms were first introduced by Bir and Pikus.[23] They are expressed by the invariants proportional to C_4 and C_5' in $\mathcal{H}^{vv}$. C_5' corresponds to the constant C_5 of Bir and Pikus, reduced by the combined $\vec{k}\cdot\vec{p}$ and strain interaction of valence and conduction band:

$$C_5'=C_5-\tfrac{2}{3}C_2P/E_g. \qquad (2)$$

This latter interaction is taken into account explicitly in $\mathcal{H}^{cv}$ and $\mathcal{H}^{cs}$ by terms weighted by C_2 and P. It causes a k-linear splitting of the conduction band and was observed by Seiler *et al.*[24] in beating effects of Shubnikov–de Haas oscillations. Howlett and Zukotynski[25] have recently discussed these effects on the conduction-band eigenstates.

In Fig. 1 the dispersion relation $E(\vec{k})$ for the uppermost ($j=\frac{3}{2}$) valence bands of InSb are shown, strain split by $T\parallel[001]$, $[111]$, and $[110]$, $T=3$ kbars. The wave vectors $\vec{k}$ are chosen from the plane perpendicular to T. The application of stress causes strong nonparabolicities, lifts the fourfold degeneracy at $\vec{k}=\vec{0}$, increases the splitting of the Kramers doublets at $\vec{k}\neq\vec{0}$ and shifts the valence-band maxima further away from the center of the Brillouin zone. As can be seen clearly, nonparabolicities occur particularly in the upper strain-split band.

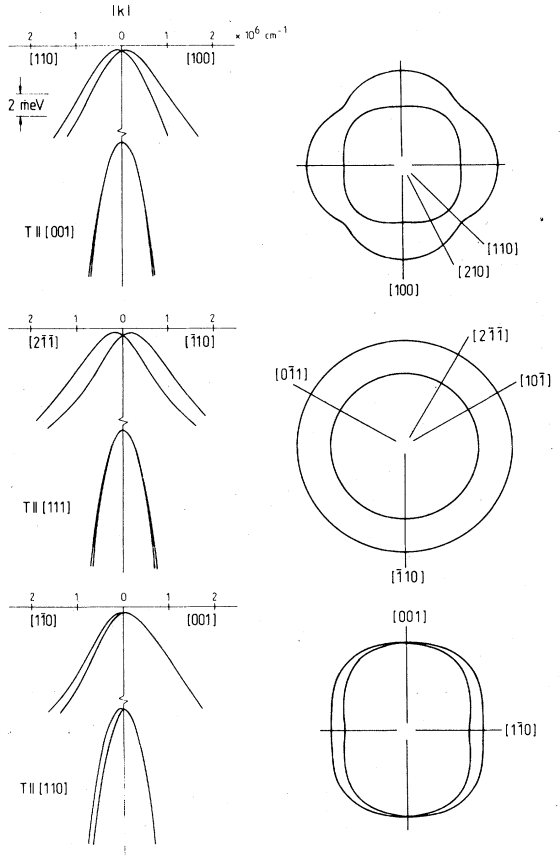

FIG. 1. Dispersion and contours of constant energy of the $j=\frac{3}{2}$ valence bands in InSb under uniaxial stress (3 kbars). The energy dispersion is shown for different directions of $\vec{k}\perp T$. The energy contours correspond to the two upper bands at an energy 6 meV below the band edge. In the scale of the figure the influence of the stress-independent k-linear terms is not resolved.

Also presented in Fig. 1 are the constant-energy contours of the two upper bands of the original quartet in the plane perpendicular to T. The energy value is 6 meV below the valence-band edge. For the geometry $T \parallel [111]$ in Ge the energy bands up to the order k^2 and ϵk are axially symmetric about this direction (Appendix A of Ref. 4). In InSb, this symmetry is not perturbed by the stress-induced k-linear terms, which also are invariant under rotations about [111] (Table VI of I). Only the normal k-linear terms exhibit the threefold symmetry of the [111] direction, but their influence is not noticeable in Fig. 1. For $T \parallel [001]$ and [110], however, the stress-induced k-linear terms produce a band splitting dependent on the direction of $\vec{k}$ and a considerable warping. From these features we conclude that: (a) in zinc-blende-type semiconductors it is not possible to obtain parabolic strain-split Γ_8 valence bands by application of uniaxial stress and hence to arrive at equally spaced Landau levels and series limits of cyclotron-resonance transitions; (b) for a description of the valence-band Landau levels under uniaxial stress an extension of the PB model may be unfavorable. The PB model starts from axially symmetric bands and treats the nonaxial terms by perturbation theory; but these grow considerably with increasing stress applied parallel to all directions except [111].

It is important to note that for $T \parallel [001]$ and [111] the stress-induced k-linear terms vanish for wave vectors parallel to the direction of stress. Consequently, if the magnetic field $\vec{H}$ is applied parallel to T, stress-induced k_H-linear terms are absent, k_H denoting the component of the wave vector along the direction of $\vec{H}$. For $T \parallel \vec{H} \parallel [110]$, however, such terms exist and possibly give rise to noncentral or k_H transitions, since in this case the extrema of the Landau-level dispersion relation (k_H dependence) are shifted linearly away from the zone center.

C. Stress dependence of Landau levels at $k_H = 0$

Introducing a standard basis for the angular momentum operators σ_i and J_i and using the cross-space matrices ρ_i, T_i, and U_i of paper I, one obtains the explicit form of the matrix Hamiltonian $\mathcal{H}$. The eigenstates of $\mathcal{H}$ are expanded into the elements of the orthonormal basis $\{|\zeta; n\alpha M\rangle\}$:

$$|\psi(\zeta)\rangle = \sum_{n\alpha M} C(\zeta; n\alpha M)\,|\zeta; n\alpha M\rangle\,,$$

which are products of spin states M of the band α, $M \epsilon \{\pm\frac{1}{2}\}$ for $\alpha \epsilon \{c, s\}$, $M \epsilon \{\pm\frac{1}{2}, \pm\frac{1}{3}\}$ for $\alpha = v$, and of harmonic oscillator states labeled by n and ζ. n denotes the oscillator quantum number and

$$\zeta = k_H/(\hbar c/eH)^{1/2}$$

the dimensionless momentum along the magnetic field. The secular matrix for the expansion coefficients C decouples into two and three submatrices for $T \parallel \vec{H} \parallel [001]$ and [111], respectively, the eigenstates of which are labeled by the quantum number P for [001] and K for [111]. For $\zeta = 0$ the secular submatrices for $T \parallel \vec{H} \parallel [001]$ and the matrix for $T \parallel \vec{H} \parallel [110]$ split into two, whose corresponding eigenstates carry the quantum number Q. If the nonaxial and tetrahedral terms of $\mathcal{H}$ are not too strong, preferably at stress $T = 0$ for low-lying levels, the states can be classified by the approximate quantum number $N_n = n + M + \frac{3}{2}$ and the parity π.

The subscript n indicates the harmonic oscillator state prevailing; n was denoted n_a in paper I.

In order to assure quick convergence, in the expansion of the magnetic eigenstates $|\psi(\zeta)\rangle$ the eight states $|\zeta; n\alpha M\rangle$ of identical quantum number N should be grouped together. Then the variational procedure, which yields the expansion coefficients C, is equivalent to aligning the Pidgeon-Brown blocks for different oscillator quantum numbers along the diagonal of a superordinate matrix and treating their mutual interaction exactly.

In Fig. 2 we show the array of the valence-band Landau levels for zero stress, $k_H = 0$, and a magnetic field of 28 kG applied along the directions [001] and [111]. The levels are classified by the sets of quantum numbers $(N_n K^\pi Q P)$ and $(N_n K^\pi)$, respectively. The sign of the energy is inverted to present hole Landau levels.

For the observation of stress-induced k-linear terms we pay special attention to the transitions indicated by arrows in Fig. 2. These are the fundamental transition $1_0 \rightarrow 2_1$ in hole cyclotron-resonance absorption (polarization vector $\vec{e}$ of the laser light perpendicular to $\vec{H}$) and the transition $2_0 \rightarrow 2_1$ in combined resonance ($\vec{e} \,|\, \vec{H}$). For the one-photon selection rules of the electron transitions (the inverse of the ones marked) see Table VIII of I.

In Figs. 3 and 4 the behavior of the lowest levels under compressive uniaxial stress is presented. All energies are referred to the energy of hole level 1_0 which usually is the lowest one. Due to the strong nonparabolic and stress-induced k-linear terms in the band structure of InSb, the level energies do not scale linearly with the magnetic field. The energies in magnetic units therefore depend explicitly on H and T and not only on the dimensionless strain-splitting constants x_u, $x_u' \propto T/H$, where

$$x_u = \epsilon_u/(\hbar e H/mc), \quad x_u' = \epsilon_u'/(\hbar e H/mc)\,,$$

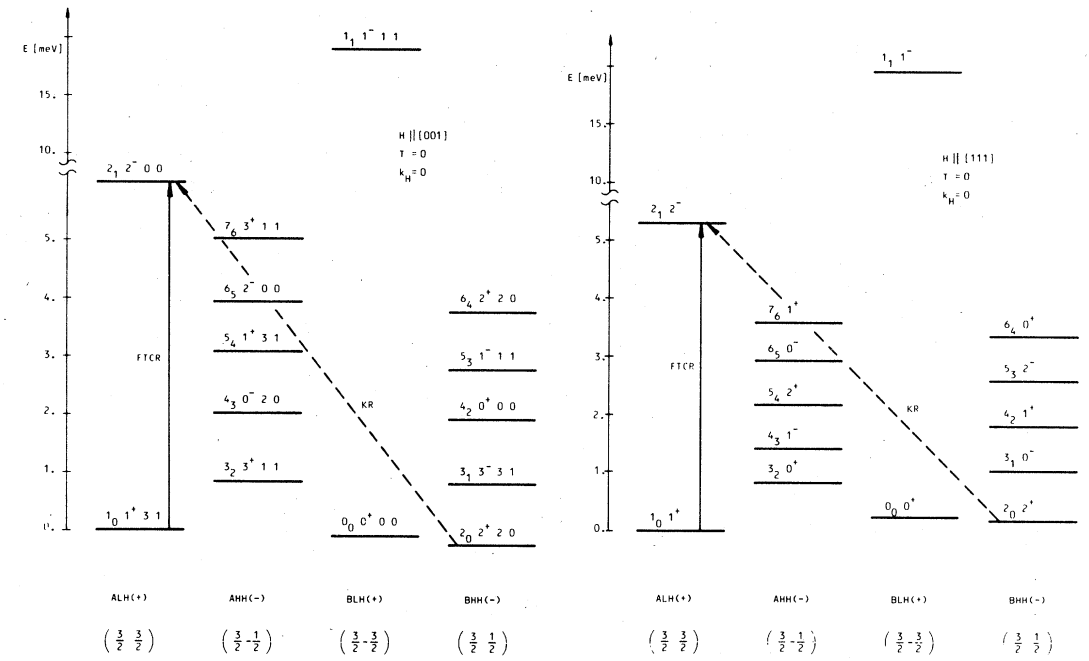

FIG. 2. Hole Landau-level scheme at $k_H=0$ and $T=0$ for $H=28$ kG in the [001] and [111] direction. FT-CR indicates the fundamental cyclotron-resonance transition and KR one combined resonance transition. Reference is made to the Pidgeon-Brown classification (cf. Ref. 18, Fig. 2).

$$\epsilon_u=\tfrac{2}{3}(s_{11}-s_{12})D_uT,\quad \epsilon_u'=\tfrac{1}{3}s_{44}D_u'T\,,$$

and s_{11}, s_{12}, s_{44} denote the cubic elastic compliance constants. In Figs. 3 and 4 the energy is drawn versus stress for a fixed magnetic field of $H=28$ kG. For $T=0$ the eigenstates are classified by N_n, for large stress by the dominant components $N_n(n,M)$. We first discuss the case $T\,\|H\,\|\,[111]$ (Fig. 3). With stress increasing, all levels move up relatively to the reference level 1_0, with exception of level 2_1 which retains an almost constant energy difference to 1_0 and is crossed frequently, exhibiting anticrossing effects with levels of quantum number $K=2$. The levels moving up most rapidly are those of the "light hole" B ladder. In Figs. 3 and 4 only one "light hole" level appears, namely, 0_0, which at about 1 kbar is separated by more than 6 meV from 1_0. At high stresses the level structure unfolds and becomes clearer. The levels of the "heavy hole" A ladder (approximate spin $M=-\frac{1}{2}$) move to higher energies almost linearly with stress, while those of the "heavy hole" B ladder ($M=+\frac{1}{2}$) are bent down. This feature is caused by the fact that pairs of levels bearing the approximate oscillator and spin quantum numbers $(n,\frac{1}{2})$ and $(n+1,-\frac{1}{2})$ repel each other due to the interaction via the stress-induced k-linear terms, thus displaying the behavior of the high-stress limit.[18] Anticrossing effects of this kind are responsible for an unexpected stress dependence of the fundamental transition $1_0\rightarrow 2_1$. Due to the repulsion between 2_0 and 2_1 the energy difference for the $1_0\rightarrow 2_1$ transition increases with stress and consequently the resonance magnetic field decreases. From Fig. 3 we also derive the stress dependence of the combined resonance transition $2_0\rightarrow 2_1$. For low stress the energy for the transition decreases, reaches a minimum at about $T=2$ kbars, and then increases. The corresponding resonance field runs through a maximum with increasing compressive stress.

For $T\,\|H\,\|\,[001]$ (Fig. 4), too, the levels of the "heavy hole" B ladder are bent down at high stresses. However, since the symmetry is changed, now the levels $(n,-\frac{1}{2})$ and $(n+1,\frac{1}{2})$ interact via the stress-induced k-linear terms. In particular the wave functions of levels 2_1 and 4_2 are mixed strongly and oscillator strength is transferred from the transition $1_0\rightarrow 2_1$ to $1_0\rightarrow 4_2$. This latter is a typical M_4-type transition in the sense of paper I, i.e., it is induced by tetrahedral terms of the Hamiltonian $\mathcal{H}$ for $k_H=0$.

Because of the anticrossing effect of levels 2_1 and 4_2 several branches are expected to be seen in the resonance field for the fundamental transition. Oscillator strength should be exchanged by the transitions $2_0\rightarrow 2_1$ and $2_0\rightarrow 4_2$ also in combined resonance. Note that in Ge the levels of the "heavy

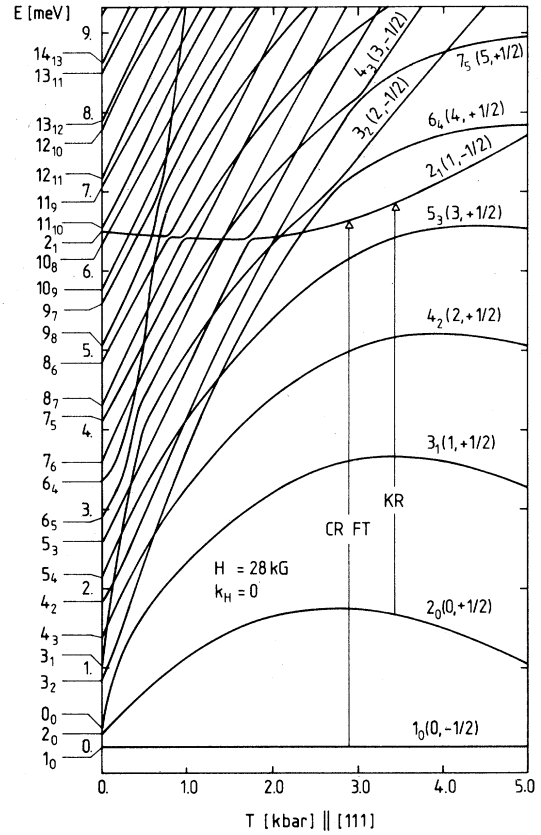

FIG. 3. Hole Landau levels at $k_H = 0$ as a function of stress $T \| [111]$. The fundamental cyclotron resonance and combined resonance transition are indicated by CR FT and KR, respectively. For the notation of the Landau levels see text.

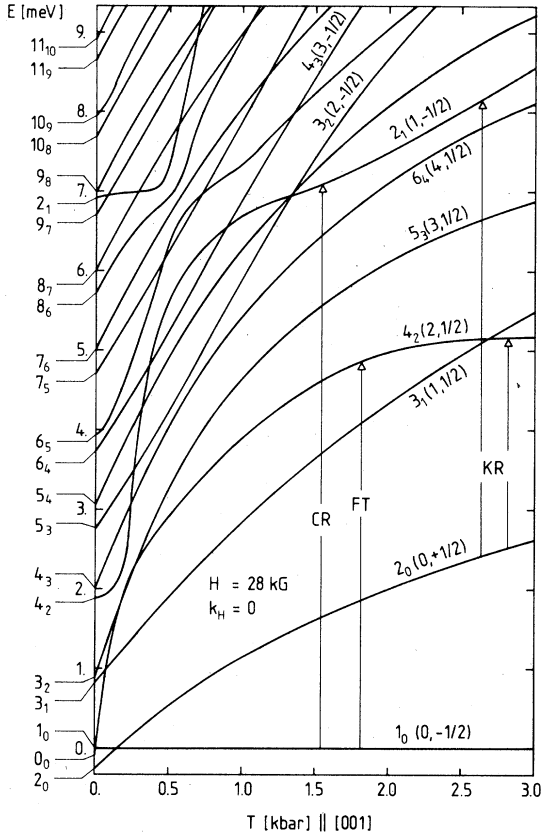

FIG. 4. Hole Landau levels at $k_H = 0$ as a function of stress $T \| [001]$ (notation as in Fig. 4). With increasing stress the fundamental cyclotron resonance transition changes from $1_0 \rightarrow 2_1$ to $1_0 \rightarrow 4_2$ as indicated.

hole" A and B ladder move almost parallel at high stresses.[5]

D. k_H dependence of the Landau levels

To demonstrate the drastic change of the Landau-level dispersion relations when stress is applied, we have drawn the level energy versus k_H for compressive stress $T = 0$ and 1 kbar in Figs. 5 and 6, respectively. In both cases the magnetic field of 28 kG is directed along [001].

For zero stress the reference level 1_0, the levels 0_0 at -0.1 meV, and 2_1 at 6.9 meV belong to the "light hole," all the other levels to the "heavy hole" ladder. To enumerate the levels we labeled them by the quantum numbers N_n at $k_H = 0$, although they change their character with increasing k_H. The only good quantum number is P. Levels drawn by the full line belong to $P = 1$, those by the broken line to $P = 0$. Anticrossing effects are observed between levels of the same P. At small values of k_H pairs of levels bearing the same number N are close together. Since both interact repulsively by terms proportional to ζ^2 the upper level of each pair shows positive, the lower, negative, curvature. This behavior and the minimum of the lower level at $k_H \neq 0$ has been predicted by Wallis and Bowlden[26] by means of a spherical model. In contrast to Ref. 26 here the B-ladder levels have negative mass, since due to warping terms these are the lower ones for $H \| [001]$.

The only level of strong parabolic dispersion is 2_1. Evidently the combined density of states for the transitions $1_0 \rightarrow 2_1$ and $2_0 \rightarrow 2_1$ has a maximum value at $k_H = 0$ and a relatively sharp line is expected to be seen in a resonance experiment, even at zero stress. At $T = 1$ kbar (Fig. 6) the levels for $k_H = 0$ are drawn asunder in agreement with Fig. 4. The dispersion of all levels has obviously become parabolic, apart from regions where levels of the same quantum number P cross. The light hole level 0_0 has moved away; the energy difference between 1_0 and 2_1 remained almost constant. There is no other maximum for the combined den-

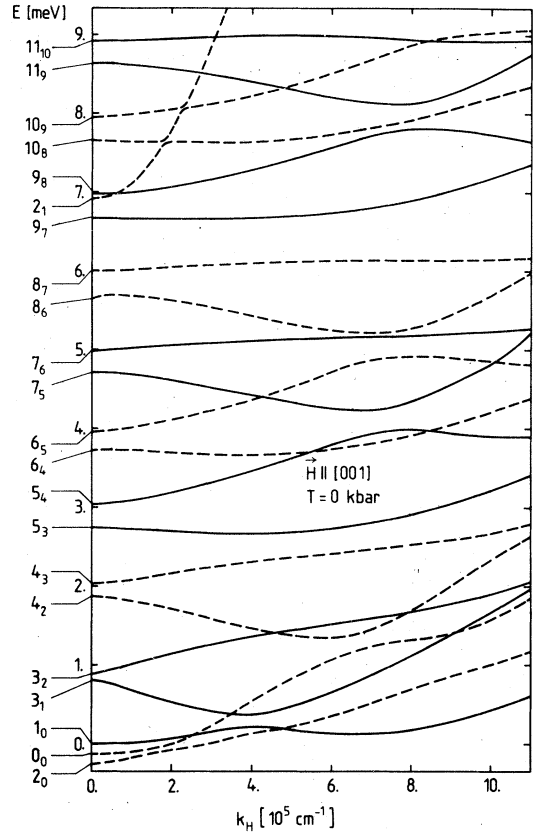

FIG. 5. k_H dependence of Landau levels for $\vec{H} \parallel [001]$ at zero stress and $H = 28$ kG. Full (dashed) lines refer to levels with quantum number $P = 1$ (0).

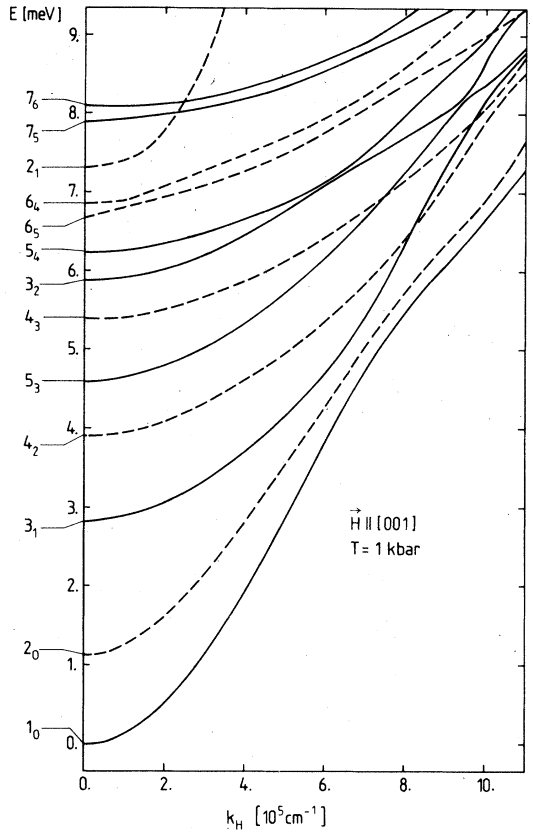

FIG. 6. k_H dependence of Landau levels for $T \parallel \vec{H} \parallel [001]$ at $T = 1$ kbar and $H = 28$ kG. Full (dashed) lines refer to levels with quantum number $P = 1$ (0).

sity of states of the transitions $1_0 \rightarrow 2_1$ and $2_0 \rightarrow 2_1$ except at $k_H = 0$. Therefore no k_H branch of the fundamental transition $1_0 \rightarrow 2_1$ exists (see Fig. 12 of Ref. 5), in contrast to Ge. Near $k_H = 10^6$ cm^{-1} there is an agglomeration of levels of different quantum numbers N which interact strongly via nonaxial terms. In that area the validity of spherical models for the band structure of InSb and of extended PB models is questionable. In calculations with negative values of k_H no asymmetry of the dispersion relations has been found, indicating that the influence of the normal k-linear term (as given in Ref. 16) is small.

The E vs k_H curves for $T \parallel \vec{H} \parallel [111]$ are similar, although the order of the nearly degenerate "heavy hole" levels of the A and the B ladders is reversed.

From Fig. 6. we conclude that for nonzero stress the intensity maxima of the resonance spectra can be fitted to a good approximation by the resonance fields for the $k_H = 0$, or central transitions, and that there is no need to resort to a line-shape fitting procedure.

III. EXPERIMENTAL METHOD

The intraband resonances were observed by measuring the straight transmission of radiation from a HCN laser through the sample as a function of magnetic field, for both up and down sweeps. The onset of a transition, as the magnetic field tunes a pair of Landau levels through the laser energy, gives rise to a minimum in the transmission. This procedure was repeated with the sample subjected to a number of different stresses, always parallel to the magnetic field, and perpendicular to the direction of propagation of the laser beam. For these Voigt configuration measurements a split-coil radial access Bitter magnet of 2-in. bore and 0.75-in. aperture was used, capable of producing 97 kG with fast sweeps (in the order of 1 min). The stress was applied with a conventional calibrated spring and lever-arm-type apparatus[27] of reduced size which fit in the tail of a Janis Varitemp exchange gas Dewar. All parts in the magnetic field were made of stainless-steel

304 or of beryllium copper. A heater wrapped around the stress frame and secured with G.E. 7031 varnish allowed us to stabilize the temperature. The stress could be determined easily to within 1%. Brass lightpipes and copper focusing cones were used to convey the radiation from the laser to the sample and from behind the sample to the Golay-cell detector.[28] The beam was chopped mechanically and the signal from the Golay cell was amplified with a PAR lock-in (JB-4 or HR8) and fed to one of two pens of an X-t chart recorder, the second pen serving to record the magnetic field to better than 0.05 kG. The HCN laser used consisted of a pyrex tube, about 10 cm in diameter and 2 m long, with mirrors at both ends to form the optical cavity. A continuous flow of gas was maintained through the tube, and an electrical discharge from one end of the tube to the other provided the pumping necessary for laser action. In order to run the laser on ammonia gas (NH_3), the inside walls of the pyrex tube were first coated with a characteristic carbon-rich brown deposit by using acetonitrile (CH_3CN) or methyl—or propyl—amine vapor [CH_3NH_2, $CH_3\times(CH_2)_2NH_2$] as a fuel for several minutes; the laser could then be run on anhydrous ammonia for many hours with stable and trouble-free output until the carbon-rich deposit on the walls became depleted. Of the many molecules present in the gas discharge the ones responsible for the laser action are those of HCN; HCN will be present in some equilibrium concentration whenever molecules containing carbon, hydrogen, and nitrogen are subjected to the rather violent conditions in the discharge, through repeated and continual dissociation and recombination. The laser can therefore be run on a variety of fuels, in addition to the ones mentioned above. The most common fuel used is a mixture of equal parts of nitrogen and methane with smaller amounts of ammonia and sometimes helium added. We chose the method described because it avoids a continuous build up in the coating of the mirrors and inside walls of the cavity which eventually would require dismantling of the laser and cleaning by hand, and second, because it avoids the need of carefully mixing different gasses before passing them into the cavity.

The continuous-flow vapor pressure was kept between 250 and 400 μm of mercury, the discharge requiring about 1500 V for currents in the order of 0.8 A. The power output was about 10 mW. The radiation was coupled out by means of a double mesh of adjustable separation to optimize the reflectivity and maximize the output on the 337-μm line. The mesh used was made of copper and had 100-μm spacing between lines. The beam was plane polarized parallel (π) or perpendicular (σ) to the magnetic field by means of a metal strip polarizer of spacing 25 μm on a mylar substrate. Polyethylene windows 0.025 in. thick were used for the laser, whereas fused or crystal quartz (with the c axis perpendicular to the plane to avoid depolarizing effects) was used for the windows of the Dewar. The samples were purchased commercially.[29] A series of low-temperature spectra with zero stress was taken with p-type scrap samples having a variety of carrier concentrations and thicknesses in order to determine the optimal conditions to observe the quantum resonances in samples of dimensions appropriate for stress work. The Zn-doped InSb finally selected had 6×10^{14} carriers cm^{-3} and a resistivity of 1.8 Ω cm at 78 K. The Ge was doped with Ga, and had 8.5×10^{14} cm^{-3} carriers, with a resistivity of 4 Ω cm. The single-crystal ingots were diamond sawed into wafers which were then string sawed into bars about $2\times2\times20$ mm. The wafers and bars were oriented to within 1° by x-ray techniques. After lapping the bars were etched in 1 part bromine, 10 methanol for InSb, and 1 part HF, 3 HNO_3 for Ge. Care was taken to avoid all traces of water in the InSb etch.

IV. EXPERIMENTAL RESULTS

A. Test measurements for Ge

In FIR experiments the resonance magnetic fields for cyclotron and combined resonances are an order of magnitude larger than in microwave experiments. The stress has to be increased by the same factor in order to perform measurements at identical dimensionless strain parameters x_u, x'_u. Due to this considerable difference in the experimental conditions, test measurements seemed to be desirable to check the setup and the theory. For this purpose the stress dependence of cyclotron-resonance absorption was measured for Ge, since precision band parameters exist for this compound from microwave experiments.[5]

To demonstrate the quality of the observed spectra we show in Fig. 7 the transmission for p-Ge, $\vec{H}\parallel T\parallel[111]$. The structure around 40 kG corresponds to the fundamental triplet $1_0\rightarrow2_1$, 5_4, 5_3 as shown in Fig. 15 of Ref. 5 where it appears at about 2.6 kG. The evolution of the fundamental $1_0\rightarrow2_1$ transition with increasing stress can be clearly seen in Fig. 7; it becomes visible as a $k_H=0$ peak at about 0.3 kbar and becomes dominant above 0.6 kbar. In Figs. 8 and 9 we present the Ge data for $\vec{H}\parallel T\parallel[111]$ and [001], respectively, in the standard plot of effective mass versus dimensionless strain parameter. In these units the present results should coincide with those of HS[5], if nonparabolicities and stress dependence of the mas-

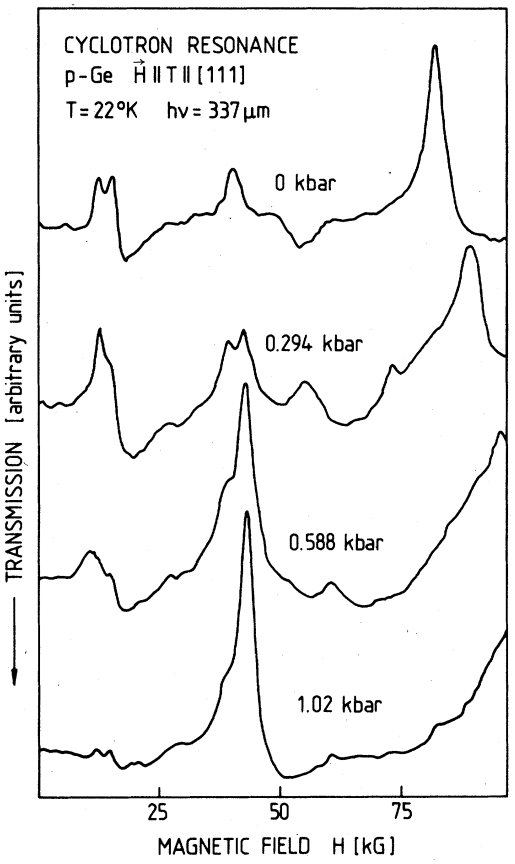

FIG. 7. CR spectrum for p-type Ge, $\vec{H} \parallel T \parallel [111]$.

ses were negligible. The difference in the light sources (far infrared of 3.679 meV here, microwaves of 0.220 meV there) shows up in some details, for instance, in the linear strain-dependent effective-mass shift of the fundamental transitions. By Eq. (25) of Ref. 5 it can be demonstrated that this shift is proportional to the resonant magnetic field and therefore much larger here than in the microwave experiment. Only a fraction of the lines seen by HS appear in our spectra. HS generated carriers by illumination of the sample with white light, we by thermal excitation of impurities. Hence doped samples were used and a temperature of 15–20 K was applied which caused broadening of the lines by k_H effects, phonon, and impurity scattering. Because the magnetic fields applied were higher, the maximum dimensionless strain parameters, which could be reached before breaking the samples, were much smaller here than in Ref. 5.

The theoretical interpretation was performed in the frame of the theory described in I, where the interaction of the three bands closest to the direct

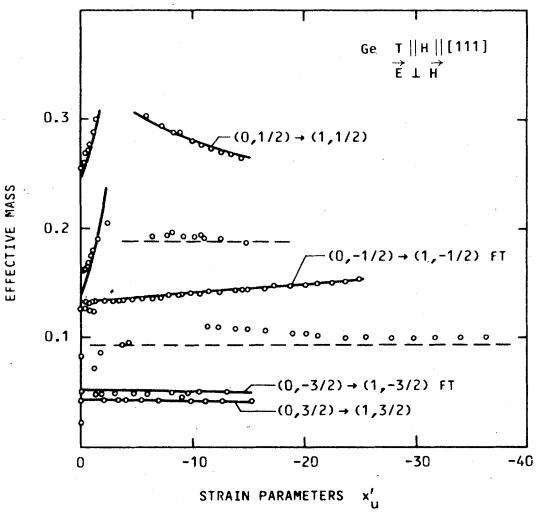

FIG. 8. Theoretical fit of CR data for p-type Ge with $\vec{H} \parallel T \parallel [111]$. ○○○ indicate peak positions in the experimental CR spectra, full lines correspond to calculated separations between Landau levels at $k_H = 0$.

gap was treated exactly. The theoretical curves in Figs. 8 and 9 were obtained with the band parameters of Ref. 5 (see Table I), i.e., without any adjustable parameters. The results are in excellent agreement with the experiment for $T \parallel \vec{H} \parallel [111]$ and far better than the interpretation with an extended PB model[10] for $H > 70$ kG. Agreement between theory and experiment is very good also for $T \parallel \vec{H} \parallel [001]$. The theoretical data were determined from Landau-level energies at $k_H \cong 0$. As seen

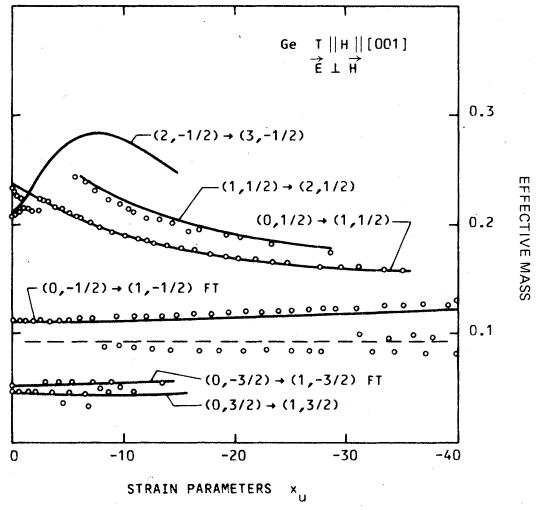

FIG. 9. Theoretical fit of CR data for p-type Ge with $\vec{H} \parallel T \parallel [001]$. ○○○ indicate peak positions in the experimental CR spectra, full lines correspond to calculated separations between Landau levels at $k_H = 0$.

in Ref. 5 there is a k_H branch of the fundamental transition $(0, -\frac{1}{2}) \rightarrow (1, -\frac{1}{2})$ with onset at $x_u = -20$. The deviations of the theoretical curve from experiment for this FT might be due to asymmetric k_H broadening. The structures not identified appear very weak and could be higher harmonics of the "classical" cyclotron resonance, the effective mass of which was taken from HS and is indicated by the broken lines. The measurements presented reaffirm the results of Hensel and Suzuki in the regime of submillimeter frequencies and provide confidence in the FIR experiments. The close agreement between our calculation and the experimental data demonstrate the capability of our theory to work well even for high magnetic fields.

B. Results for InSb

Cyclotron resonance (CR) and combined resonance (KR) spectra were measured for $\vec{H} \parallel T \parallel [111]$, [001], [110], [112], and for various stress values.[10] In this paper only data for the [111] and [001] directions will be discussed and interpreted with the theory developed in I. For the less-symmetric [110] and [112] directions strong k_H effects are expected, and the low symmetry prevents a reduction of the secular problem for $k_H \neq 0$ so that a

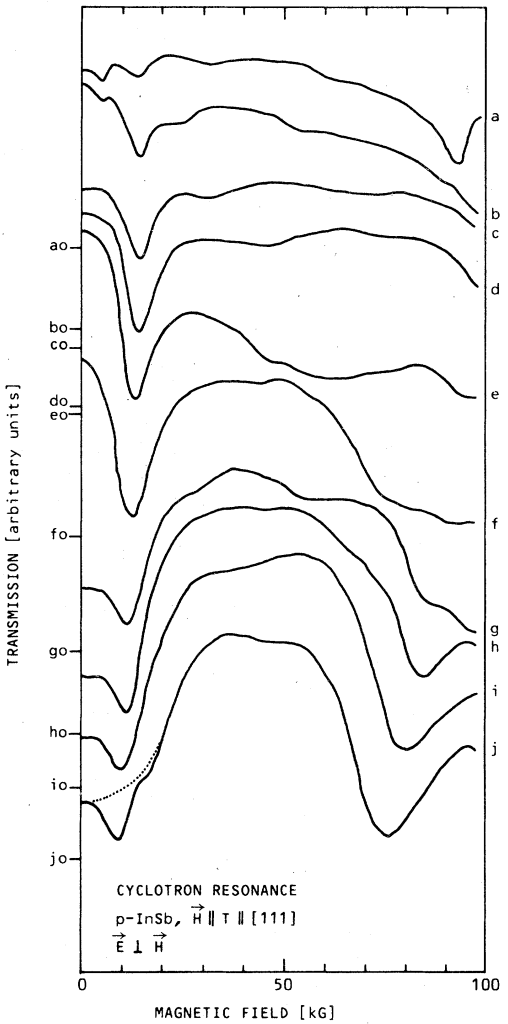

FIG. 10. CR spectra for InSb with $\vec{H} \parallel T \parallel [111]$. The different spectra correspond to the stress values (in kbar): (a) (0), (b) (0.595), (c) (1.13), (d) (2.08), (e) (2.60), (f) (2.94), (g) (3.41), (h) (3.65), (i) (4.18), and (j) (4.77). The level of zero transmission is indicated for each spectrum.

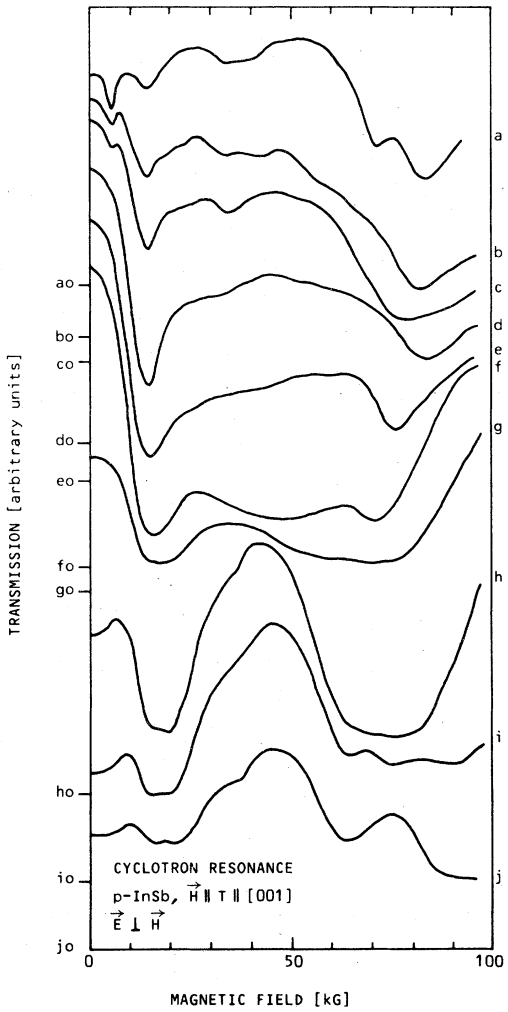

FIG. 11. CR spectra for InSb with $\vec{H} \parallel T \parallel [001]$. The different spectra correspond to the stress values (in kbar): (a) (0), (b) (0.19), (c) (0.34), (d) (0.78), (e) (1.22), (f) (1.59), (g) (1.77), (h) (1.95), (i) (2.13), and (j) (2.34). The level of zero transmission is indicated for each spectrum.

quantitative interpretation of these data in the frame of our theory would have consumed more computer time than seemed worthwhile. The [110] and [112] directions in fact only provide a cross check, and no new parameters. Experimental spectra for the high-symmetric stress directions are presented in Figs. 10–12. From these we extract the resonance magnetic field of peak positions as function of the applied stress as shown in Figs. 13–16. According to the discussion in Sec. IID these data correspond to the energy differences between Landau levels at $k_H = 0$.

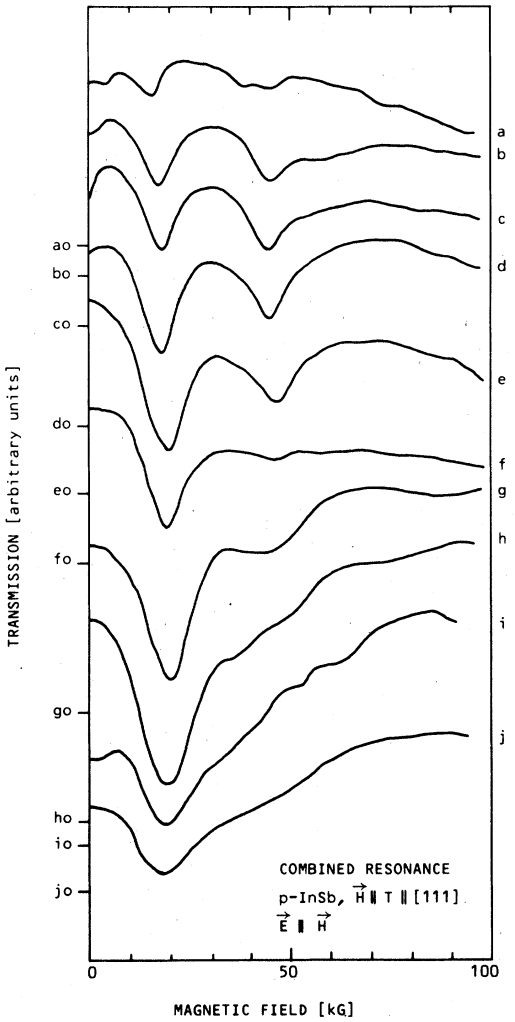

FIG. 12. Combined resonance (KR) spectra for InSb with $\vec{H} \parallel T \parallel [111]$. The different spectra correspond to the stress values (in kbar): (a) (0), (b) (0.41), (c) (0.60), (d) (0.79), (e) (1.13), (f) (1.33), (g) (1.70), (h) (2.08), (i) (2.28), and (j) (2.61). The level of zero transmission is indicated for each spectrum.

1. $T \parallel H \parallel [111]$

The most important line arises from the fundamental transition $1_0 \rightarrow 2_1$. We therefore have drawn the peak positions of this line in an enlarged scale in Fig. 14 for all runs performed. The line can be traced to $T = 0$. At low stresses the effective mass of the transition is $(\gamma_1 - \gamma_3)^{-1}$ to zeroth order. In Ge the corresponding line is almost stress independent with a small linear-strain-dependent shift. In InSb the levels 2_0 and 2_1 strongly repel each other with increasing stress due to the stress-induced k-linear terms, as seen in Fig. 3. Consequently the resonance field decreases in accord with the experimental data. The rate of decrease is very sensitive towards variations of C_5.

The k-linear interaction also influences the stress dependence of the resonance field for the transition $2_0 \rightarrow 2_1$ in combined resonance. In contrast to Ge, where the resonance field for this transition increases monotonically,[10] it is bent down in InSb at approximately 2 kbars. This characteristic feature agrees with experiment; the differences in the absolute field values, however, are probably due to experimental difficulties, because the line broadens and fades away at rather

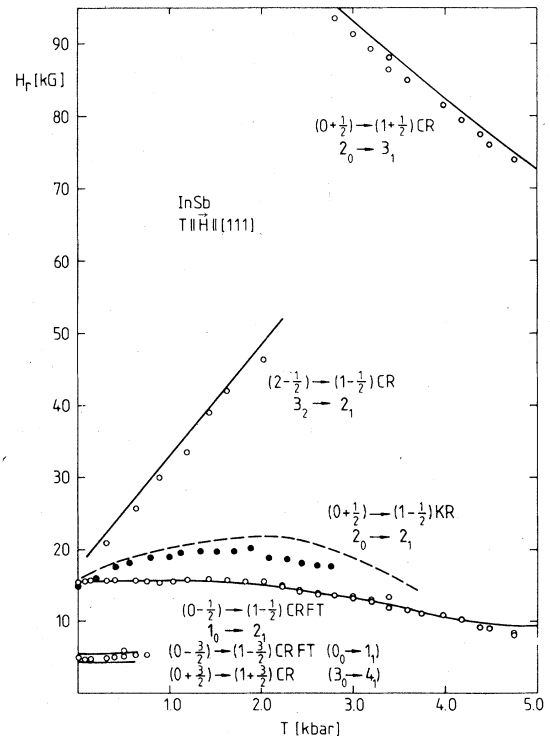

FIG. 13. General structure of the CR (experiment: ○, theory: ——) and KR (experiment: ●, theory: ---) data for p-type InSb with $\vec{H} \parallel T \parallel [111]$.

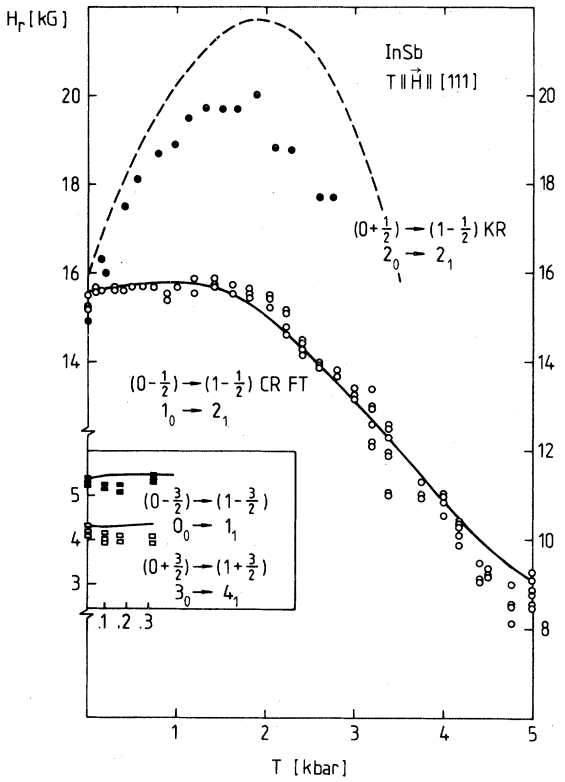

FIG. 14. Details of the CR (experiment: ○, □, ■, theory: ——) and KR (experiment: ●, theory: ---) data for p-type InSb with $\vec{H} \parallel T \parallel [111]$.

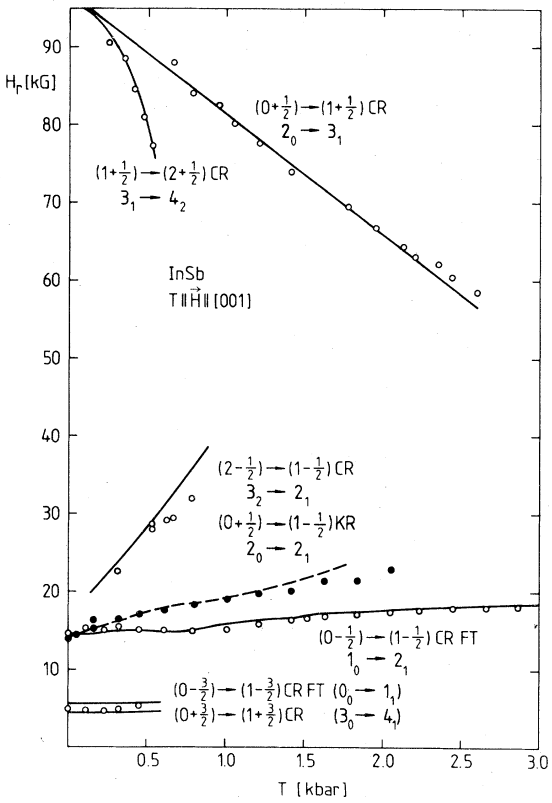

FIG. 15. Gross structure of the CR (experiment: ○, theory: ——) and KR (experiment: ●, theory: ---) data for p-type InSb with $\vec{H} \parallel T \parallel [001]$.

low stresses. The diminuition of intensity is consistent with theory, since combined resonance results from the high degree of mixing of the $M = \pm\frac{1}{2}$ and $M = \pm\frac{3}{2}$ components of the $j = \frac{3}{2}$ multiplet; stress weakens the mixing because of the removal of the degeneracy.

At low fields the theory predicts resonances for the light hole transitions $0_0 \rightarrow 1_1$ and $3_0 \rightarrow 4_1$.

The two transitions are not resolved, actually, as indicated in Fig. 13. A crude line-shape fit for the different runs from superpositions of Lorentzians lead to the results drawn in the lower part of Fig. 14. In zeroth order the effective mass for the fundamental transition $0_0 \rightarrow 1_1$ is $(\gamma_1 + \gamma_3)^{-1}$.

Further cyclotron-resonance transitions identified are $3_2 \rightarrow 2_1$ and $2_0 \rightarrow 3_1$. Their resonance field is very sensitive to variations of the deformation potential D_u'. Also small changes of the differences between γ_1^L, γ_2^L, and γ_3^L appreciably alter the field values for the transition $2_0 \rightarrow 3_1$. These fields are very high. Their determination by calculations within the $j = \frac{3}{2}$ manifold showed insufficient results and divergence, when the perturbation series was extended to third order, and made the application of the three-band Kane model indispensible.

2. $T \parallel H \parallel [001]$

The behavior of the fundamental transition $1_0 \rightarrow 2_1$ is more complex for the geometry $T \parallel \vec{H} \parallel [001]$ and the interpretation of the experimental data follows other lines than previously assumed.[17] The anticrossing effects in the stress dependence of the Landau levels (Fig. 4) also become evident in the resonance fields. The resonance field of the transition $1_0 \rightarrow 2_1$, which tends to remain almost stress independent, is crossed by that of the M_2-type transition $1_0 \rightarrow 6_5$ at about 0.5 kbar and of the M_4-type transition $1_0 \rightarrow 4_2$ at 1.5 kbar. Repulsion occurs at the first cross point due to the warping interaction, at the second due to the interaction via stress-induced k-linear terms, and leads to several branches of the fundamental transition (dotted lines in Fig. 16). Oscillator strength for the transition is large at the horizontal parts and diminishes with increasing distance thereof.

Because the linewidth of the transitions is broad (Sec. IV A) at the crosspoints the different branches cannot be resolved. For each stress value we therefore calculated the resonance field by super-

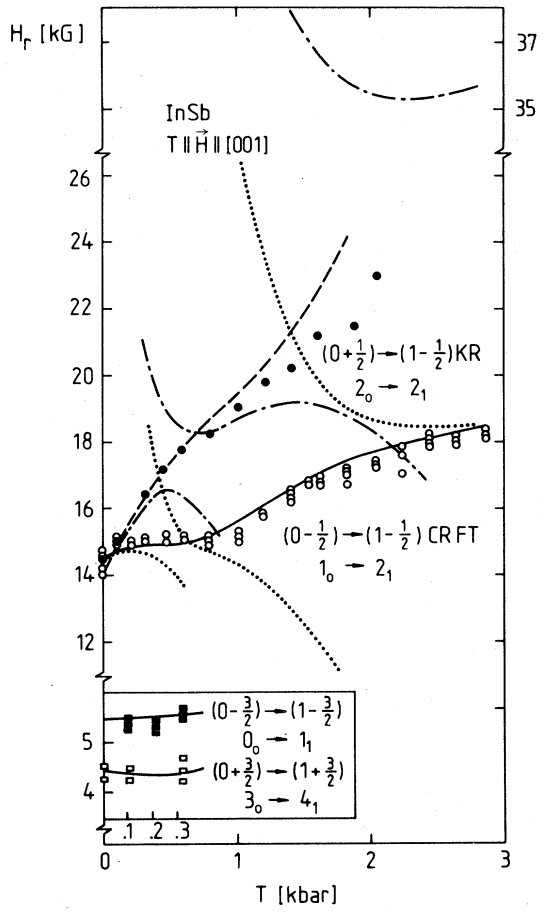

FIG. 16. Details of the CR (experiment: ○, □, ■, theory: ——) and KR (experiment: ●, theory: ---) data for p-type InSb with $\vec{H} \| T \| [001]$. The stress dependence of the KR (CR) data result from a combination of transitions between three pairs of Landau levels indicated by -•- (•••••) as described in the text.

position of Lorentzians, which were centered at the sites of the different branches and weighted by the oscillator strengths of the transitions (full line).

The agreement with the experimental data (open circles) is very good. The resonance field at high stress values (3 kbars) is very sensitive to variations of the constant C_4.

Similarly the resonance field for the transition $2_0 \rightarrow 2_1$ in combined resonance is affected strongly by level crossings. Tending to increase monotonically it is crossed by the field values of the $2_0 \rightarrow 6_5$ and $2_0 \rightarrow 4_2$ transitions and follows the dash-dotted line. Superposition of Lorentzians at the different branches weighted by the respective oscillator strengths (dashed line) agrees well with the experimental points (full circles).

While the effective mass for the $1_0 \rightarrow 2_1$ transition is approximately $(\gamma_1-\gamma_2)^{-1}$, the one for the $0_0 \rightarrow 1_1$ fundamental transition is $(\gamma_1+\gamma_2)^{-1}$. The resonance field of the latter and of the transition $3_0 \rightarrow 4_1$ is found (resolved analytically) in Fig. 16. In the higher field regime, transitions $3_2 \rightarrow 2_1$, $2_0 \rightarrow 3_1$, and $3_1 \rightarrow 4_2$ can be seen. These depend sensitively on the deformation potential D_u.

A series of further lines at intermediate field values has not been identified. They might be noncentral or impurity transitions. These small peaks were of no consequence in the analysis of the data and were not investigated further.

3. *Determination of parameters*

Compared to the work on Ge[5] a much larger number of parameters is involved in the computations of Landau levels in InSb. The parameter values obtained from an optimum fit to the experiment are presented in Table I. In order to reduce the number of adjustable parameters, we made use of some relations from $\vec{k} \cdot \vec{p}$ theory. Because of the small gap the effective mass of the Γ_1 conduction band is almost entirely determined by the interaction with the uppermost spin-orbit split Γ_5 valence bands.[33] We therefore neglected A'. Consistently the relation[34]

$$P = [\tfrac{1}{3}(3+\gamma_1^L+4\gamma_2^L+6\gamma_3^L+6\kappa^L+\tfrac{3}{2}q)(\hbar^2 E_g/2m)]^{1/2} \quad (3)$$

was used between the momentum matrix element P, the gap energy, and the Luttinger parameters. We furthermore used the approximation[34]

$$\kappa^L = -\tfrac{1}{3}(\gamma_1^L - 2\gamma_2^L - 3\gamma_3^L + 2) - \tfrac{1}{2}q \quad (4)$$

by neglecting the $\vec{k} \cdot \vec{p}$ interaction of the band-edge valence states with the remote conduction bands of Γ_4 symmetry.

The values of E_g, Λ, B, C, the cubic elastic compliance constants, and the deformation potentials were taken from the literature. The deformation potentials had to be modified within the experimental error bars in order to reproduce the linear strain-dependent shift of the high-field "heavy hole" resonances.

The Luttinger parameters γ_1^L, γ_2^L, γ_3^L were determined so as to yield agreement with the experimental values for the fundamental transitions and for a good overall fit. The experimental error bars give rise to some uncertainty in the fitting parameters. We therefore present a range of possible values for the Luttinger parameters. With sets outside of these limits no fit was possible. q was taken from Pidgeon and Groves.[16]

Finally the constants C_4 and C_5 were determined from the deviations of the FT $1_0 \rightarrow 2_1$ from the horizontal line. Their order of magnitude is confirmed by pseudopotential calculations[35] which gave the

TABLE I. Band parameters used for an optimum fit of the theoretical model to the experiment; for C_4 and C_5 the relation to previously used notations[17] is indicated.

	InSb		Ge (Ref. 5)
E_g	= 0.235 eV (Ref. 15)		0.889 eV
Λ	= 0.803 eV (Ref. 19)		0.287 eV
A'	= 0 eV cm^2		0 eV cm^2
γ_1^L	= 40.1 ± 1.5		13.38
γ_2^L	= 18.1 ± 0.7		4.24
γ_3^L	= 19.2 ± 0.7		5.69
κ^L	= 17.0 ± 0.7		3.41
q^L	= 0.39 (Ref. 16)		0.06
C	= 9.32×10^{-11} eV cm (Ref. 16)		0
P	= 9.97×10^{-8} eV cm		$9.97\cdot10^{-8}$ eV cm
B	= 12.6×10^{-16} eV cm^2 (Ref. 24)		0
s_{11}	= 2.261×10^{-3} kbar^{-1} (Ref. 30)		0.955×10^{-3} kbar^{-1}
s_{12}	= -0.764×10^{-3} kbar^{-1}		-0.262×10^{-3} kbar^{-1}
s_{44}	= 3.180×10^{-3} kbar^{-1}		1.458×10^{-3} kbar^{-1}
$C_1 - D_d$	= −7.0 eV (Ref. 22)		−11.00 eV
D_u	= 2.90 eV (Refs. 31, 32)		3.32 eV
D_u'	= 4.10 eV (Refs. 31, 32)		3.81 eV
C_2	= 3.0 eV		0
C_4	= 1.13×10^{-7} eV cm	$(=\frac{2}{3}C)$	0
C_5	= 10.33×10^{-7} eV cm	$(=\frac{2}{3}B)$	0

values $C_4 = 0.85\cdot10^{-7}$ eV cm and $C_5 = 5.12\cdot10^{-7}$ eV cm. $C_2 = 2$ eV as taken from the work of Seiler *et al.*[24] appears to be too small, since the value for C_5', which for $T \parallel [111]$ characterizes the strain interaction of the Γ_5 valence band with all but the lowest conduction band turns out to be too large from relation (2). We used a value of 3 eV, but the spectra are not very sensitive to changes of C_2.

V. CONCLUDING REMARKS

The study of quantum resonances under uniaxial stress in the valence bands of semiconductors of the diamond–zinc-blende family yields detailed information on the intrinsic band parameters, e.g., effective-mass values and deformation potentials. This information is obtained, however, only by use of a theory that takes into consideration the experimental conditions (strength of the magnetic field) and the peculiarities of the energy bands (band gaps, k-linear terms). It has been shown in this paper that quantum resonances in p-type InSb observed in an FIR experiment can be quantitatively understood in the frame of a theory that takes into account all magnetic and strain couplings which are possible due to the tetrahedral symmetry of the zinc-blende lattice. Due to the high magnetic fields of these measurements, the coupling between the top valence band and the lowest conduction band, the stress-induced nonparabolicities, and the warping terms have to be taken into account exactly, which means that the PB theory in its extended version[10] (including stress) and the theory of Suzuki and Hensel are of limited validity here.

The results presented in this paper recommend the FIR technique for investigating the Landau levels in zinc-blende-type materials and at the same time prove the strength of the theory of paper I in describing these experiments. Concerning the quantitative results of this paper a comment on the band parameters is in place. Interpretations of previous interband magneto-optical experiments,[15,16] but also of the recent very detailed photoconductivity measurements,[12] based on the PB model, lead to Luttinger inverse mass parameter, which are 25% smaller than those obtained in this paper. More recently, however, the reinterpretation of the interband data by Weiler[36] showed that inclusion of excitonic effects in the PB model, even in a simplified version, results in an increase of the band parameters of PB by 20%. It must be left to future investigations whether a more detailed inclusion of excitonic effects and a more accurate consideration of the tetra-

hedral terms in the discussion of interband data can solve the discrepancy in the band parameters.

ACKNOWLEDGMENTS

The authors have benefited from discussions with many colleagues, whose contributions to the field is given in the references. We would like to thank Dr. R. Grisar and Professor G. Bauer for sending a report of their results prior to publication and to Dr. P. Vogl for providing a PB computer program. Experimental work was performed at the Francis Bitter Magnet Laboratory, MIT, Cambridge, Mass. Work has been supported in part by the NSF.

---

*Present address: Instituto des Pesquisas Espaciais, Conselho Nacional de Desenvolvimento, Cientifico e Tecnologico, 12200 S. J. Campos, S. P. Brazil.
†Present address: City College of CUNY, New York, N. Y. 10031.
‡Present address: Brooklyn College, CUNY, Brooklyn, N. Y. 11210.

[1]J. M. Luttinger and W. Kohn, Phys. Rev. 97, 869 (1955).
[2]J. M. Luttinger, Phys. Rev. 102, 1030 (1956).
[3]J. C. Hensel and K. Suzuki, Phys. Rev. Lett. 22, 838 (1966).
[4]K. Suzuki and J. C. Hensel, Phys. Rev. B 9, 4184 (1974).
[5]J. C. Hensel and K. Suzuki, Phys. Rev. B 9, 4219 (1974).
[6]D. M. S. Bagguley, M. L. A. Robinson, and R. A. Stradling, Phys. Rev. Lett. 6, 143 (1963).
[7]M. L. A. Robinson, Phys. Rev. Lett. 17, 963 (1966).
[8]H. T. Tokver and G. Ascarelli, *Proceedings of the Ninth International Conference on the Physics of Semiconductors, Moscow*, 1968 (Publishing House, "NAUKA", Leningrad, 1968), p. 326.
[9]K. J. Button, B. Lax, and C. C. Bradley, Phys. Rev. Lett. 21, 350 (1968).
[10]R. Ranvaud, Ph.D. thesis, Brown University, 1973 (unpublished).
[11]R. Ebert, H. Pascher, G. Appold, and H. G. Häfele, Appl. Phys. 14, 155 (1977).
[12]R. Grisar, H. Wachernig, G. Bauer, J. Wlasak, J. Kowalski, and W. Zawadzki, Phys. Rev. B 18, 4355 (1978).
[13]G. E. Pikus and G. L. Bir, Sov. Phys. Solid State 1, 1502 (1959) [Fiz. Tverd.Tela (Leningrad) 1, 1642 (1959)].
[14]W. H. Kleiner and L. M. Roth, Phys. Rev. Lett. 2, 334 (1959).
[15]C. R. Pidgeon and R. N. Brown, Phys. Rev. 146, 575 (1966).
[16]C. R. Pidgeon and S. H. Groves, Phys. Rev. 186, 824 (1969).
[17]R. Ranvaud, F. H. Pollak, U. Rössler, and H.-R. Trebin, *Proceedings of the Thirteenth International Conference on the Physics of Semiconductors, Rome 1976*, edited by F. G. Fumi (Tipografia Marves, Rome, 1976), p. 1171.
[18]H.-R. Trebin, U. Rössler, and R. Ranvaud, Phys. Rev. B 19, 686 (1979) (preceding paper).
[19]R. L. Aggarwal, in *Semiconductors and Semimetals*, edited by R. K. Willardson and A. C. Beer (Academic, New York, 1972), Vol. 9, p. 151.
[20]E. O. Kane, J. Phys. Chem. Solids 1, 249 (1956).
[21]G. Dresselhaus, Phys. Rev. 100, 580 (1955).
[22]R. L. Bell and K. T. Rogers, Phys. Rev. 152, 746 (1966).
[23]G. L. Bir and G. E. Pikus, Sov. Phys. Solid State 3, 2221 (1962) [Fiz. Tverd. Tela (Leningrad) 3, 3050 (1961)].
[24]D. G. Seiler, B. D. Bajaj, and A. E. Stephens, Phys. Rev. B 16, 2822 (1977).
[25]W. Howlett and S. Zukotynski, Phys. Rev. B 16, 3688 (1977).
[26]R. R. Wallis and H. J. Bowlden, Phys. Rev. 118, 456 (1960).
[27]F. H. Pollak and M. Cardona, Phys. Rev. 172, 816 (1968).
[28]Unicam Industries, Cambridge, England.
[29]The Ge was bought from Sylvania Electric Products Co., Towanda, Pennsylvania, and the InSb from Cominco American Inc., Spokane, Washington.
[30]R. F. Potter, Phys. Rev. 103, 47 (1956).
[31]C. Benoit á la Guillaume and P. Lavallard, J. Phys. Soc. Jpn. 21, Suppl. 288 (1966).
[32]F. H. Pollak and J. Halpern, Bull. Am. Phys. Soc. 14, 433 (1968).
[33]C. Hermann and C. Weisbuch, Phys. Rev. B 15, 823 (1977).
[34]See Ref. 26 of paper I.
[35]H.-R. Trebin, M. Cardona, R. Ranvaud, and U. Rössler, *Proceedings of the III International Conference on the Physics of Narrow-Band Gap Semiconductors, Warsaw, 1977*, edited by J. Rouluszkiewcz, M. Gorska, and E. Kaczmarek-Moraviec (North-Holland, Amsterdam, 1978), p. 227.
[36]M. H. Weiler, J. Magn. Magn. Mater. 11, 131 (1978).